A Nitroxide Derivative as a Probe for Conformational Studies of Short Linear Peptides in Solution. Spectroscopic and Molecular Mechanics Investigation

Basilio Pispisa,*,‡ Antonio Palleschi,§ Lorenzo Stella,‡ Mariano Venanzi,‡ and Claudio Toniolo#

Dipartimento di Scienze e Tecnologie Chimiche, Università di Roma Tor Vergata, 00133 Roma, Italy, Dipartimento di Chimica, Università di Roma La Sapienza, 00185 Roma, Italy, and Centro di Studio sui Biopolimeri, C.N.R., Dipartimento di Chimica Organica, Università di Padova, 35131 Padova, Italy

Received: March 9, 1998; In Final Form: June 16, 1998

The photophysics of linear Aib-based hexapeptides (Aib = α-aminoisobutyric acid) of general formula Ac-Toac-$(Aib)_n$-Trp-$(Aib)_r$-O*t*Bu (TnTrp), where $n + r = 4$, and Toac and Trp are a nitroxide spin labeled $C^{\alpha,\alpha}$-disubstituted glycine and tryptophan, respectively, were investigated in methanol and dioxane solutions by steady-state and time-resolved fluorescence measurements. Another hexapeptide, i.e., Boc-(S)Bin-Ala-Aib-Toac-$(Ala)_2$−O*t*Bu (T-Bin), carrying the same nitroxide derivative and a binaphthyl as the fluorophore was also studied by the same techniques. Quenching of the excited tryptophan or binaphthyl chromophore proceeds on a time scale from subnanoseconds to a few nanoseconds, depending on the conformers distribution in solution. CD and IR spectral patterns in methanol or $CDCl_3$ suggest that the backbone of the peptides examined is in the 3_{10}-helical conformation, thus preserving the structural features of the crystal state, as earlier determined by X-ray diffraction measurements. The fluorescence results were satisfactorily described by a dipole−dipole interaction mechanism, in which electronic energy transfer takes place from the excited tryptophan or binaphthyl to Toac, provided the mutual orientation between the fluorophore and Toac is taken into account. This implies that interconversion among conformational substates is slow on the time scale of the transfer process. Molecular mechanics calculations coupled with time decay data allowed us to build up the most probable structures of these peptides in methanol solution.

Introduction

Extensive work has been carried out for understanding the mechanism through which excited states are quenched by paramagnetic species, such as nitroxyl radicals, but there is not yet a univocal interpretation of the phenomenon.[1−3] Apart from the intrinsic interest, the importance of these studies currently stems from the capability of the doublet quencher to probe the structural and dynamic features of membranes,[4,5] micelles,[6,7] and proteins surface.[1] In addition, unlike many free radical species, •NO displays selective reactivity, the major biological targets including heme−iron and iron−sulfur proteins.[8] Very recently, the rate constant for the reaction of nitroxide with tryptophan and tyrosine radicals in peptides and proteins was measured, suggesting that •Trp and •Tyr are likely and important targets for •NO generated in vivo.[9]

Among the nitroxide derivatives currently used, Toac is a nitroxide spin-labeled $C^{\alpha,\alpha}$-disubstituted glycine (Chart 1) that, when incorporated into a peptide chain, provides a means of restricting the range of backbone conformations.[10,11] Indeed, besides favoring stereochemical rigidity, Toac is able to probe 3_{10}/α-helix conformations in peptides doubly labeled at appropriate relative positions.[12]

In the research program aimed at elucidating the dynamics and conformational features of polypeptides[13] and linear oligopeptides[14] in solution by studying the photophysical behavior of these materials carrying suitable fluorophores, we have recently investigated short linear peptides containing tryptophan (Trp) and Toac (T), and (*S*)-binaphthyl (Bin) and Toac (Chart 1). The general formula for the former series of peptides is Ac-Toac-$(Aib)_n$-Trp-$(Aib)_r$-O*t*Bu, where Ac is acetyl, O*t*Bu *tert*-butoxy, Aib α-aminoisobutyric acid, and $n + r = 4$, hereafter denoted as TnTrp, namely T0Trp, T1Trp, T2Trp, and T3Trp, to emphasize the length of the spacer between the chromophores in the hexapeptides. In the latter case, the formula is Boc-(S)-Bin-Ala-Aib-Toac-$(Ala)_2$−O*t*Bu, denoted as T-Bin, where Boc is *tert*-butyloxycarbonyl, and Ala L-alanine.

CHART 1

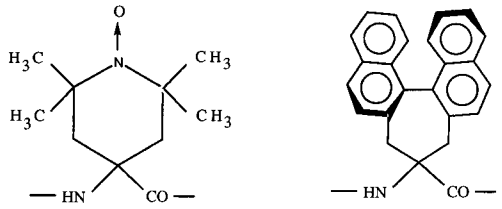

According to X-ray diffraction results,[15,16] in the crystal state the backbone of the peptides examined is in the 3_{10}-helical conformation, with right-handedness (r.h.) for TnTrp, and left-handedness (l.h.) for T-Bin. This latter structure is unusual for a peptide containing L-alanine residues, and is most probably due to the presence of the chiral (*S*)-binaphthyl moiety. Chart 2 illustrates the crystal state structures of T-Bin and T3Trp peptides, the former comprising two conformers, here denoted as a and b, differing from each other by the different puckering of the Toac moiety and its spatial orientation with respect to the binaphthyl group.

‡ Università di Roma Tor Vergata.
§ Università di Roma La Sapienza.
# Università di Padova.

S1089-5647(98)01415-1 CCC: $15.00
Published on Web 09/15/1998

CHART 2: Ball−Stick Representation of X-ray Diffraction Structures of T-Bin, Comprising Two Conformers (a and b), and T3Trp Hexapeptides

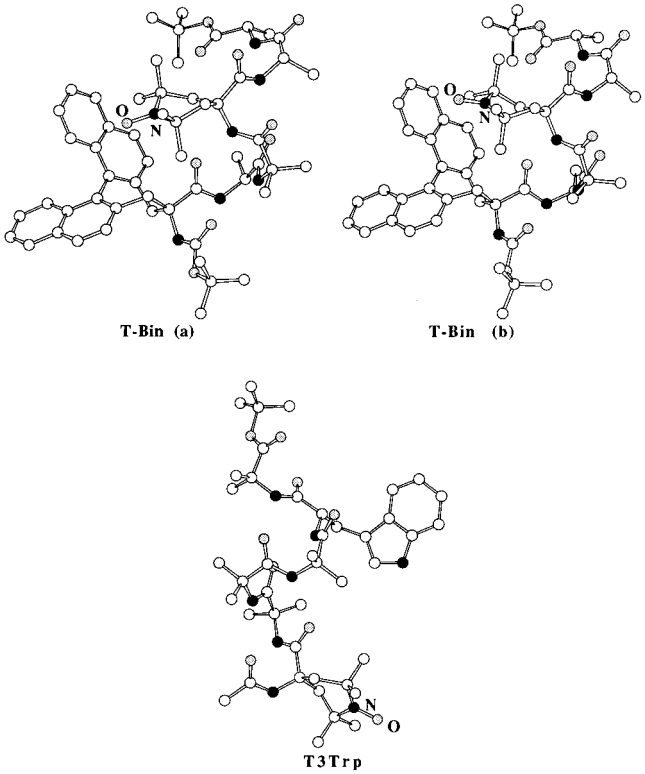

CHART 3: Schematic Representation of a Tryptophan Residue for Defining the Geometry of Its Internal Rotation[a]

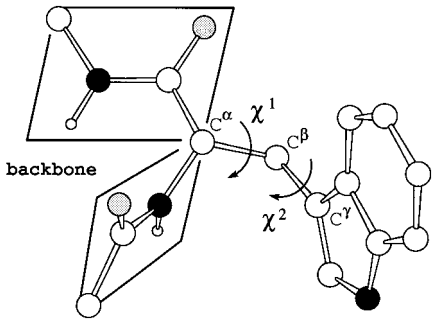

The two side-chain dihedral angles χ^1 and χ^2 are shown.

To ascertain whether the ordered structure of the crystal state is preserved in solution, and to investigate the conformational equilibria that characterize the TnTrp peptides, owing to the rotation around the dihedral angles χ^1 and χ^2 of the Trp side chain shown in Chart 3, we have undertaken a spectroscopic investigation, based on steady-state and time-resolved fluorescence experiments, and on IR and CD spectral data, as well. The spectroscopic results, coupled with those obtained by molecular mechanics calculations, allow us to conclude that, irrespective of the polarity of the solvents used, the peptides examined maintain the basic features of the crystal state, and exhibit a poor flexibility in solution.

Experimental Section

Materials. The terminally protected hexapeptide Boc-(S)-Bin-Ala-Aib-Toac-$(Ala)_2$−O*t*Bu (T-Bin) was synthesized by solution methods and fully characterized.[16] Bin and Toac residues were incorporated using the *N*-ethyl,*N*′-(3−dimethylamino−propyl)carbodiimide/1-hydroxy-7-aza-benzotriazole approach, while Ala and Aib residues were incorporated via the symmetrical anhydride method. The sequence following Toac was built up using fluoren-9-ylmethoxycarbonyl N^α-protection. The Ac-Toac-$(Aib)_n$-Trp-$(Aib)_r$-O*t*Bu peptide series ($n + r = 4$) was prepared as described above for the T-Bin hexapeptide. However, in Ac-Toac-$(Aib)_3$-Trp-Aib-O*t*Bu the -$(Aib)_3$- stretch was inserted in a single step using the 5-oxazolone method.

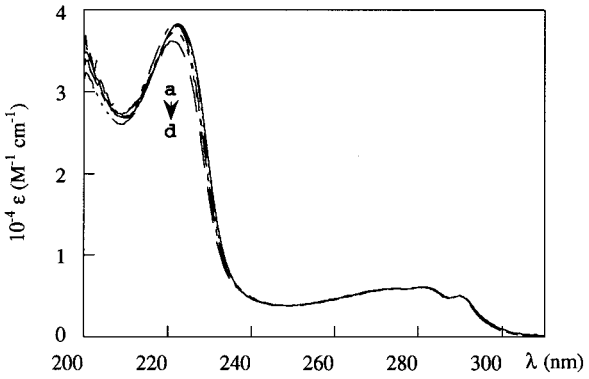

Figure 1. UV absorption spectra of the TnTrp peptides in methanol (curves a → d correspond to $n = 0 \rightarrow 3$). The sum spectrum of 2Trp and Toac is also reported for comparison (full line).

Methods. Steady-state fluorescence spectra were recorded on a SPEX Fluoromax spectrofluorometer, operating in SPC mode. Quantum yields were obtained by using Trp in water (298 K, pH 7.2) as reference: $\Phi_0 = 0.14 \pm 0.02$. Nanosecond decays were measured by a CD900, SPC lifetime apparatus from Edinburgh Instruments. Excitation in the UV region was achieved by ultrapure hydrogen as filling gas (300 mmHg), fwhm = 1.2 ns, 30 kHz repetition rate. The decay curves were fitted by a nonlinear least-squares analysis to exponential functions by an iterative deconvolution method. All experiments were carried out in quartz cells, using solutions previously bubbled for 20 min with ultrapure nitrogen.

Absorption and IR spectra were recorded on a Jasco 7850 and a Perkin-Elmer 983 spectrophotometer, respectively, the latter using CaF_2 cells. Circular dichroism (CD) measurements were performed on a Jasco J-600 instrument with appropriate quartz cells.

Other apparatuses have already been described.[14]

Results and Discussion

Absorption, CD, and IR Spectra. The UV absorption spectra of TnTrp peptides in methanol or dioxane are quite similar to the sum spectrum of Toac and tryptophan, as shown in Figure 1. The same is true for T-Bin, in the sense that the presence of Toac in the molecule does not perturb the absorption spectrum of binaphthyl, as illustrated in Figure 2A. In the latter case, however, the electronic spectrum of Bin and T-Bin exhibit a shift to 305 nm of the naphthalene band at 280 nm, while the band at around 225 nm is split in two components centered at 220 and 232 nm (Figure 2A). According to Förster,[17] these findings are suggestive of a strong electronic coupling of naphthyl moieties in the ground state via intramolecular exciton interaction.[18a]

Circular dichroism spectra of TnTrp (Figure 3) and T-Bin (Figure 2B) hexapeptides are poorly diagnostic about the conformational tendencies of these compounds. The usually informative far-UV region (190−250 nm) is dominated by the contributions of the Bin,[19a] Toac,[12c] and Trp[19b] chromophores which strongly overlap those of the peptide chromophore, but

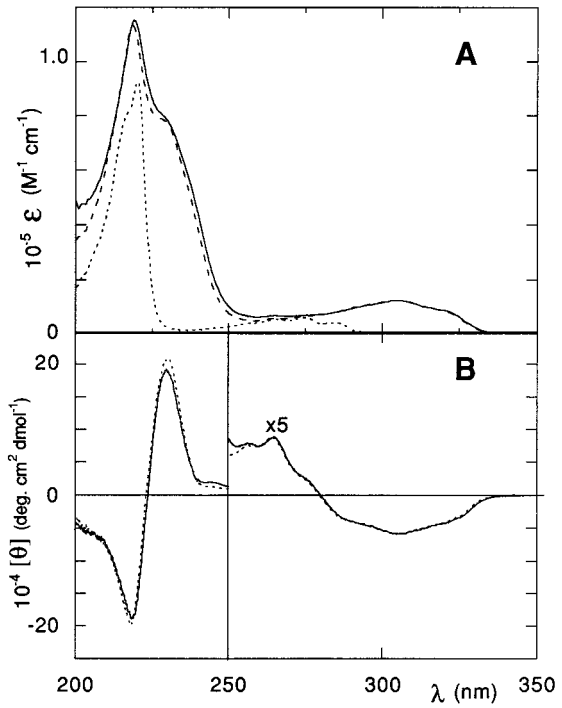

Figure 2. Absorption (A) and circular dichroism (B) spectral patterns of Bin (broken line), T-Bin (full line), and naphthalene (dotted line) in methanol.

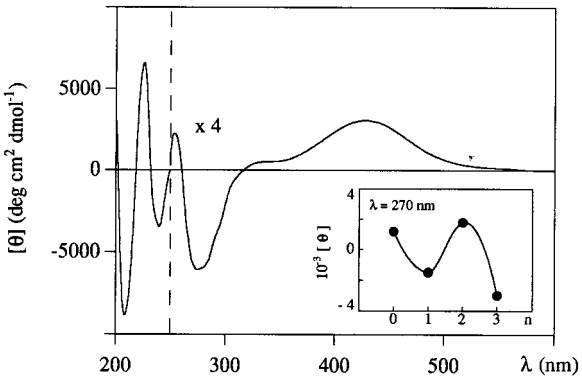

Figure 3. CD spectrum of T1Trp in methanol. Insert: variation of the ellipticity of tryptophan at 270 nm as a function of the number of Aib residues in the spacer. The helix periodicity is easily recognizable.

there is a tendency of the aromatic (Trp) side chains to give rise to positive rotational strength in the 210−230-nm region. On the other hand, the CD spectrum of T-Bin in methanol shows an exciton splitting in the same wavelength region, as illustrated in Figure 2B, in full agreement with the foregoing absorption results. In the visible region Toac exhibits extrinsic positive ellipticity at around 430 nm, which varies depending on the relative position of Trp in the backbone ([Θ] = 300/800 deg·cm^2·dmol^{-1}). There is no clear correlation, however, with the helical periodicity, but the intensity of tryptophan band at 270 nm shows a trend reflecting such a periodicity as the number of Aib residues in the spacer increases (insert of Figure 3).

We next investigated the infrared spectra of the peptides in $CDCl_3$, under conditions of appropriate dilution that minimize self-association. Intermolecular H-bonding interactions are thus negligible for all peptides at concentrations around 10^{-4} M.

The band in the amide-A region at 3430 cm^{-1} can be assigned to the stretching mode of free peptide N−H group, while the stretching mode in the frequency range 3340−3320 cm^{-1} can be assigned to intramolecularly hydrogen-bonded N−H groups. In addition, the band at around 3475 cm^{-1} in the TnTrp peptides is ascribable to the N−H group of tryptophan.

Where the integrated intensities of the bands of H-bonded (A_b) and free (A_f) N−H groups at around 3340 and 3430 cm^{-1}, respectively, were calculated, the ratio A_b/A_f, normalized for the appropriate extinction coefficients, was found to be approximately 1.7−1.8 for all TnTrp peptides and 1.9 for T-Bin. In view of the experimental errors, these figures are in satisfactory agreement with the theoretical value of 2 for a hexapeptide in the 3_{10}-helical conformation, because the hydrogen-bonding scheme is of the $i \rightarrow i + 3$ type, thus implying the occurrence of four intramolecular H-bonded N−H groups.

On the basis of the foregoing data, it is reasonable to conclude that all peptides examined preserve in solution the ordered structure already present in the crystal state, very likely maintaining the same helical screw sense, too.

Steady-State and Time-Resolved Fluorescence. It is generally accepted that one of the major pathways of nitroxide quenching of singlet states is the intersystem crossing to the triplet induced by electron exchange,[1a,2] or an internal conversion to ground state,[3] both mechanisms being not mutually exclusive. In other instances, however, charge transfer[1c,20] or Förster energy transfer[17] were found to be important.[1b,5b] Calculations based on measured spectral properties showed that Förster transfer mechanism extends the nitroxides' quenching radius to as much as 10 Å,[5b] so that the range of the induced quenching is considerably over what it would be with only vibrational coupling or enhanced intersystem crossing. On the other hand, Dexter energy transfer[21] requires singlet energies greater than the lowest excited-state energy of the nitroxide, besides a short center-to-center distance, less than, say, 4.5 Å.[18b] In the present case the singlet energies are $E_{00,Trp} = 4.13$ eV and $E_{00,Bin} = 3.73$ eV, while the energy of the lowest excited state of Toac is around 2.9 eV. The Dexter mechanism is hence feasible, provided the interprobe distance is short enough.

Steady-state fluorescence in methanol and dioxane shows a substantial quenching of Trp or naphthalene singlet emission by Toac in TnTrp and T-Bin peptides, respectively, as illustrated in Figure 4. No evidence for exciplex emission could be found, however, even by decreasing solvent polarity from methanol to dioxane. The fluorescence quantum yield (Φ) of TnTrp and T-Bin in the two solvents are reported in Table 1, together with the efficiency of the quenching process, E, as given by $[1 - (\Phi/\Phi_0)]$, where Φ_0 is the quantum yield of 2Trp or Bin.

As far as the time decay measurements are concerned, the decay curves of 2Trp and Bin ($\lambda_{ex} = 290$ and 305 nm, $\lambda_{em} =$ 350 and 360 nm, respectively) were found to be strictly monoexponential; e.g., τ_0 is 5.8 and 4.9 ns in methanol, and 6.2 and 3.6 ns in dioxane, respectively. As expected, the τ_0 values of Bin are definitely smaller than that of naphthalene ($\tau_N = 52.5 \pm 0.7$ ns), indicating a strong dynamic quenching due to the aforementioned coupling regime.

The fluorescence decay of TnTrp and T-Bin peptides could be well-fit to a sum of three exponentials in the former case, dominated by the first short-lived component, and of two exponentials in the latter, i.e.:

$$I(t) = \sum_m \alpha_m \exp(-t/\tau_m) \qquad (1)$$

where m goes from 1 to 3 for TnTrp and from 1 to 2 for T-Bin. A typical example of the decay curves is presented in Figure 5 for 2Trp, T1Trp, Bin, and T-Bin. In all cases, no significant change was observed on varying the sample concentration within 1 order of magnitude ($1 \times 10^{-6} - 2 \times 10^{-5}$ M), so that interchain effects can be ruled out.

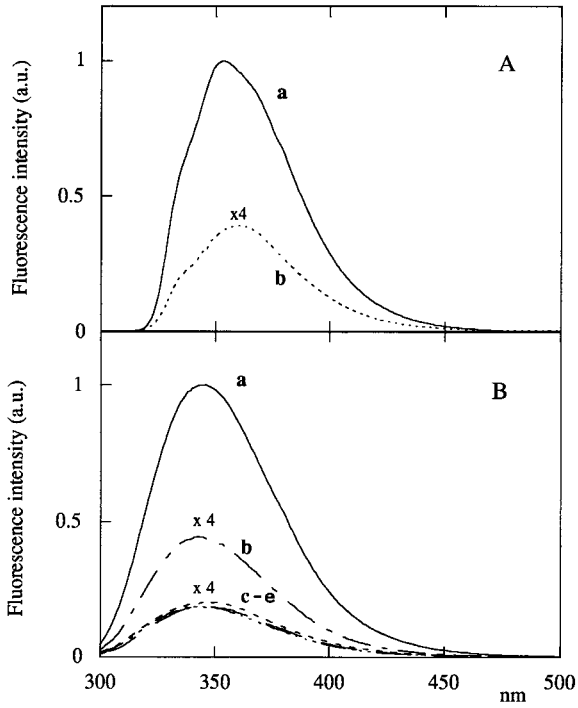

Figure 4. Steady-state fluorescence spectra of (A) Bin (a) and T-Bin (b), and (B) 2Trp (a), T1Trp (b), T0Trp (c), T2Trp (d), and T3Trp (e) peptides in methanol.

TABLE 1: Quantum Yields and Quenching Efficiencies from Steady-State Fluorescence Measurements[a]

	methanol		dioxane	
peptide	Φ	E^b	Φ	E^b
T0Trp	0.02	0.95	0.05	0.93
T1Trp	0.05	0.89	0.06	0.91
T2Trp	0.02	0.95	0.06	0.92
T3Trp	0.02	0.95	0.09	0.88
T-Bin[c]	0.07	0.90	0.07	0.91

[a] $\lambda_{ex} = 290$ nm for TnTrp and 305 nm for T-Bin. [b] Quenching efficiency, $E = 1 - (\Phi/\Phi_0)$, where Φ is the quantum yield of Trp in the samples and $\Phi_0 = 0.49 \pm 0.06$ (methanol) and 0.72 ± 0.03 (dioxane) that in 2Trp. [c] The quantum yield of Bin is $\Phi_0 = 0.71$ (methanol) and 0.77 (dioxane).

Table 2 lists the lifetimes, pre-exponents, and quenching efficiencies for TnTrp peptides in methanol and dioxane, whereas Table 3 lists the same parameters for T-Bin in different solvent media, the quenching efficiency being always given by:

$$E_{m,\mathrm{exp}} = 1 - (\tau_m/\tau_0) \qquad (2)$$

Owing to the high purity of the samples examined, we can rule out the presence of contaminants and attribute each decay component to one conformer populating the solution, as shown below.

Because the distance and orientation of the nitroxide with respect to the indole in TnTrp hexapeptides varies, depending on the number of Aib residues in the spacer, molecular mechanics calculations were employed to gather information on the geometric and steric constraints that control both these parameters.[14c,d,22] Briefly, we started by putting the backbone chain of TnTrp in the r.h. 3_{10}-helix, in agreement with both IR and X-ray results, and by fixing initially the dihedral angle $\chi^2 = 90°$ and $-90°$, corresponding to the two energy minimum conformations, perpendicular and antiperpendicular,[23] and the dihedral angle $\chi^1 = 60°$, $-60°$, and 180° for the rotamers g^+, g^-, and t, respectively (Chart 3). Because the backbone chain bonds attached to C^α, with positions defined by the ϕ,ψ dihedral angles ($\phi = -60°$, $\psi = -30°$ for r.h. 3_{10}-helix), perturb the rotation of the side-chain $C^\alpha-C^\beta$ bond, owing to the interactions with the atoms near C^γ,[24,25] we searched for the total energy in the deepest minimum of the *m*th conformer by eq 3. It comprises stretching and bending terms (STR and BEN), besides electrostatic (COUL), nonbonding (NB), and torsional (TOR) potentials similar to those previously employed by us,[14,25] i.e.:

$$U_{m,\mathrm{tot}} = \mathrm{COUL} + \mathrm{NB} + \mathrm{TOR} + \mathrm{STR} + \mathrm{BEN} \qquad (3)$$

In the case of T-Bin we followed the same procedure, but we put the backbone in l.h. and r.h. 3_{10}-helix, to explore both conformations of the main chain. Owing to the rigidity of this hexapeptide, we expected a very narrow distribution of conformers for each backbone structure, as it was indeed the case (see below).

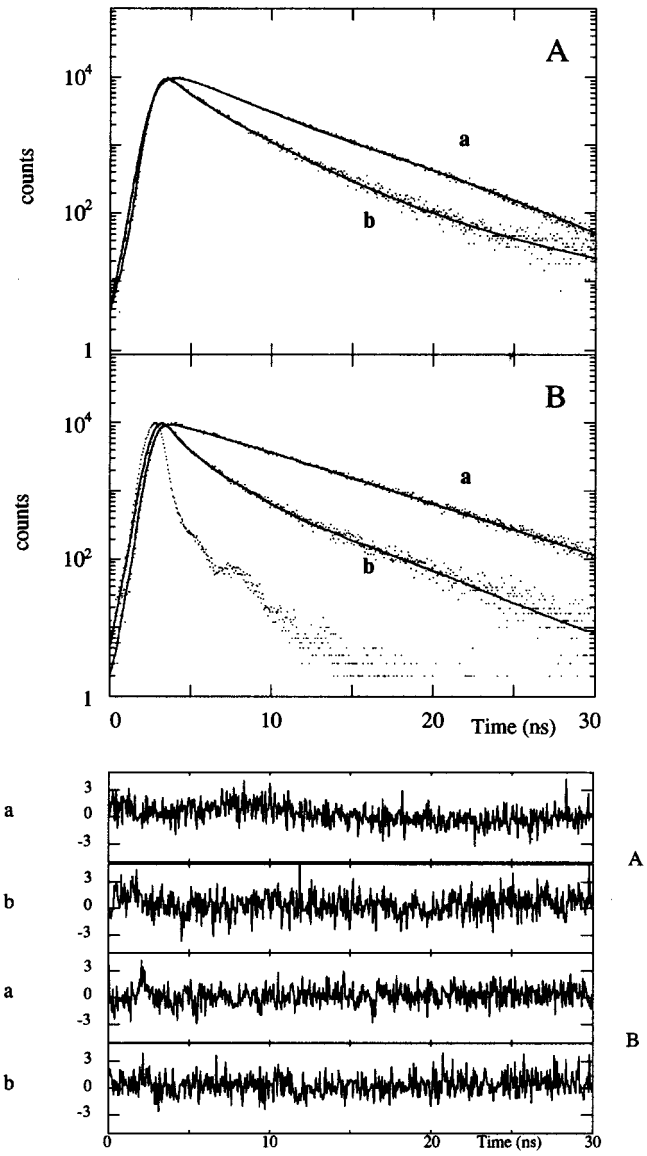

Figure 5. Typical example of fluorescence decays. Normalized decay profile of (A) Bin (a) and T-Bin (b) ($\lambda_{ex} = 305$, $\lambda_{em} = 360$ nm), and (B) 2Trp (a) and T1Trp (b) ($\lambda_{ex} = 290$, $\lambda_{em} = 350$ nm) in methanol. The full lines represent the best fit to the experimental data by a monoexponential for Bin and 2Trp, a two-exponential for T-Bin, and a three-exponential for T1Trp decay. The lamp profile is also shown in (B), and the residuals at the bottom of the plots.

TABLE 2: Fluorescence Lifetimes and Quenching Efficiencies of TnTrp Peptides[a]

	methanol										dioxane									
sample	α_1	τ_1 (ns)	E_1[b]	α_2	τ_2 (ns)	E_2[b]	α_3	τ_3 (ns)	E_3[b]	χ^2	α_1	τ_1 (ns)	E_1[b]	α_2	τ_2 (ns)	E_2[b]	α_3	τ_3 (ns)	E_3[b]	χ^2
T0Trp	0.86	0.25	0.96	0.11	0.84	0.86	0.04	5.0	0.14	1.1	0.85	0.09	0.99	0.13	1.72	0.72	0.02	5.1	0.18	1.1
T1Trp	0.86	0.41	0.93	0.12	0.96	0.83	0.02	5.2	0.10	1.1	0.75	0.32	0.95	0.19	1.89	0.69	0.06	4.9	0.21	1.2
T2Trp	0.56	0.30	0.95	0.30	1.90	0.68	0.14	5.4	0.06	1.1	0.73	0.35	0.94	0.18	2.41	0.61	0.09	5.6	0.10	1.1
T3Trp	0.80	0.20	0.96	0.16	1.70	0.71	0.04	4.6	0.21	1.0	0.44	0.31	0.95	0.33	2.10	0.64	0.23	3.9	0.33	1.2

[a] $\lambda_{ex} = 290$, $\lambda_{em} = 350$ nm. Fluorescence time decay of 2Trp: $\tau_0 = 5.8$ ns (methanol, $\chi^2 = 1.0$) and 6.2 ns (dioxane, $\chi^2 = 1.1$). Uncertainties: in lifetimes around 8% for the long and medium component and around 50% for the shortest one, in the pre-exponents around 20%. Even relatively large errors in τ do not significantly affect the calculated quenching efficiency, E, when its value is near 1. For instance, for the 90-ps lifetime in T0Trp in dioxane, $\Delta E/E \approx 1\%$ for $\Delta\tau/\tau = 50\%$. In the other cases, the uncertainty in E is around 10%. [b] From eq 2.

TABLE 3: Fluorescence Lifetimes and Quenching Efficiencies of T-Bin in Different Solvents[a]

solvent	τ_0[b] (ns)	α_1	τ_1 (ns)	E_1[c]	α_2	τ_2 (ns)	E_2[d]	χ^2
methanol	4.89	0.79	1.36	0.72	0.21	4.46	0.07	1.33
ethanol	4.55	0.75	1.01	0.78	0.25	3.90	0.15	1.13
2-propanol	4.12	0.79	0.53	0.87	0.21	3.25	0.21	1.19
1-butanol	4.12	0.63	0.68	0.83	0.37	3.15	0.24	0.99
ethyl acetate	3.95	0.59	0.95	0.73	0.41	3.48	0.09	1.14
dioxane	3.62	0.55	0.84	0.77	0.45	3.06	0.15	1.28

[a] $\lambda_{ex} = 305$, $\lambda_{em} = 360$ nm. The uncertainty in lifetimes is better than 10%, while that of the pre-exponents is around 20%. [b] Fluorescence time decay of Bin. [c] From eq 2. The uncertainty is around 10%. [d] From eq 2, the uncertainty being about 30%.

To overcome the uncertainty in the absolute value of the total energy, arising from the empirical terms of eq 3, we used eq 4, where ΔU_m is the difference between the energy of the mth conformer, $U_{m,tot}$, and the lowest energy among all conformers of each peptide, U_{min}, which plays the role of a reference energy.

$$\Delta U_m = U_{m,tot} - U_{min} \tag{4}$$

As a result, the probability of the mth conformer was evaluated by eq 5:

$$P_m = \exp(-\Delta U_m/RT)/\sum_m \exp(-\Delta U_m/RT) \tag{5}$$

where the sum is over all conformers of the given peptide.

The most relevant computational results are summarized in Tables 4 and 5 for TnTrp and T-Bin, respectively, where the calculated quenching efficiency is that given by eq 6, according to the dipole−dipole interaction model. The reason of this choice shall be apparent shortly.

$$E_{m,calcd} = \frac{1}{1 + \left[\frac{2}{3\kappa_m^2}\left(\frac{R_m}{R_0}\right)^6\right]} \tag{6}$$

In eq 6 R_m is the center-to-center distance of the probes in the mth conformer, κ_m^2 the corresponding orientation parameter, and R_0 the distance at which 50% transfer of excitation energy occurs, namely:[14]

$$R_0 = 9.79 \times 10^3[(^2/_3\Phi_0 J_F)/n^4]^{1/6} \tag{7}$$

where Φ_0 is the quantum yield of the 2Trp or Bin, n the refractive index of the solvent, and J_F ($cm^2 \cdot mol^{-1}$) the overlap integral calculated from fluorescence spectra, as given by eq 8:

$$J_F = \frac{\int_0^\infty F_D(\bar{\nu})\epsilon_A(\bar{\nu})\,\bar{\nu}^{-4}\,d\bar{\nu}}{\int_0^\infty F_D(\bar{\nu})\,d\bar{\nu}} \tag{8}$$

where $F_D(\bar{\nu})$ is the fluorescence intensity of the donor (tryptophan or binaphthyl) and $\epsilon_A(\bar{\nu})$ the extinction coefficient of the acceptor (Toac) at wavenumber $\bar{\nu}$. From the spectral patterns, the overlap integral in methanol is 6.21×10^{-18} $M^{-1} \cdot cm^3$ for TnTrp and 6.10×10^{-18} $M^{-1} \cdot cm^3$ for T-Bin, and hence R_0 is 9.3 and 9.7 Å, respectively.

Where the donor and acceptor groups do not rotate fast enough to randomize their orientation during the donor lifetime, a relative orientation between the nitroxide and Trp or Bin in the hexapeptides can be evaluated by eq 9,[14b,d,26] i.e.:

$$k_m^2 = \cos^2\theta(3\cos^2\gamma + 1) \tag{9}$$

Chart 4 exemplifies the spatial geometry of the transition dipole moments of the two moieties in T-Bin,[26] where R' is the distance between the centers of mass of Bin and Toac, the transition dipole moment of Toac, lying in the CNC plane,[2b] being taken perpendicularly to the NO bond, while that of binaphthyl as a vectorial combination of the dipoles from each naphthalene. The angle that the transition dipole moment of Bin makes with the line joining the center of mass of Bin and Toac is denoted as γ, while **E** is the vector representing the electric field at the center of mass of Toac induced by the transition dipole moment of Bin, and θ the angle between **E** and the transition dipole moment of Toac.[14b,26] By contrast, when the chromophores are freely rotating the isotropic average value of the orientation parameter, $\langle\kappa_m^2\rangle = 2/3$, is used.

In Chart 4, the total dipole moment of the 3_{10}-helical backbone, directed from the N-terminus to the C-terminus, is also shown. It generates an electrostatic potential[27] that, in principle, could affect the coupling of the transition moments of the probes.[28] However, this is not the case here because the total dipole moment of the helical peptide forms an angle with respect to the transition moment of Toac very close to 90°.

In the case of TnTrp peptides, the scheme is similar to that shown in Chart 4. The transition dipole moment of Trp coupled with that of Toac was chosen to be ^1L_a[29a] because by using ^1L_b the computed κ_m^2 parameter leads to a very poor agreement between calculated and observed efficiency. This finding is consistent with recent theoretical and experimental data,[29b] indicating that in polar solvent media, such as methanol, the emitting state is ^1L_a.

The main inference to be drawn from Tables 4 and 5 is that, using the relative energies of the sterically most favored conformers to estimate the Boltzmann probability, P_m, of each conformer, the agreement between P_m and the lifetimes pre-exponent, α_m, is satisfactory.[30] This latter quantity measures the relative population of the species undergoing energy transfer, which, in turn, depends on the structural features of the molecule. In addition, where the interprobe distance and orientation parameter of the minimum energy conformers were employed to estimate transfer efficiency, E_m (eq 6), the agreement between these values and those experimentally observed (eq 2) is very good, as one can infer by comparing

TABLE 4: Molecular Parameters of TnTrp Conformers and Calculated and Experimental Quenching Efficiency in Methanol

peptide	ΔU_m[a] (kcal/mol)	R_m[b] (Å)	κ^2_m[c]	P_m[d]	α_m[e]	$E_{m,\mathrm{calcd}}$[f]	$E_{m,\mathrm{exp}}$[g]
T0Trp	0	6.50	1.032	0.75	0.86, 0.09, 0.06	0.93	0.96, 0.86, 0.14
	1.28	7.47	1.390	0.09		0.89	
	1.42	9.76	0.025	0.07		0.03	
	1.44	9.27	0.374	0.07		0.36	
	2.40	5.74	0.063	0.01		0.63	
	2.42	8.76	0.210	0.01		0.32	
T1Trp	0	6.62	1.648	0.81	0.86, 0.12, 0.02	0.95	0.93, 0.83, 0.10
	1.16	10.09	1.895	0.12		0.64	
	1.70	9.87	0.200	0.05		0.17	
	2.52	10.81	0.764	0.01		0.32	
	2.95	7.72	0.054	0.01		0.20	
	3.00	8.75	0.385	0.00		0.45	
T2Trp	0	5.73	0.571	0.60	0.56, 0.30, 0.14	0.94	0.95, 0.68, 0.06
	0.38	6.02	0.068	0.32		0.58	
	1.86	7.41	0.046	0.03		0.21	
	1.92	7.40	0.074	0.02		0.31	
	1.98	7.33	0.846	0.02		0.84	
	2.82	6.82	0.002	0.01		0.02	
T3Trp	0	6.52	1.052	0.83	0.80, 0.16, 0.04	0.93	0.96, 0.71, 0.21
	1.27	10.77	0.961	0.10		0.37	
	1.54	7.10	0.039	0.06		0.23	
	2.71	6.60	0.843	0.01		0.91	
	3.43	7.79	0.328	0.00		0.59	
	5.40	9.73	0.002	0.00		0.00	

[a] From eq 4. [b] Center-to-center distance between Toac and Trp. [c] From eq 9. [d] From eq 5. [e] Lifetime pre-exponents, from Table 2, to be compared with the figures of the preceding column [f] From eq 6. [g] From eq 2, to be compared with the figures of the preceding column.

TABLE 5: Structures of T-Bin in Methanol in the Deepest Energy Minimum

backbone conformation[a]	ΔU_{tot}[b] (kcal·mol^{-1})	R_m[c] (Å)	$k_m{}^2$[d]	$E_{m,\mathrm{calcd}}$[e]	$E_{m,\mathrm{exp}}$[f]
l.h. 3_{10}-helix[g]	0	5.84	0.090	0.74	0.72,0.07
	0	6.18	0.004	0.07	
r.h. 3_{10}-helix	1.7	8.69	0.760	0.67	

[a] Left-hand (l.h.) and right-hand (r.h.) helix. [b] From eq 4, where U_{min} refers to the two isoenergetic conformers with main chain in the l.h. 3_{10}-helix. [c] Interprobe center-to-center distance. [d] From eq 9. [e] From eq 6. [f] From eq 2, $m = 1$ and 2 (see Table 3). [g] See Figure 8.

the figures of the last two columns in Table 4 for TnTrp and by the plot of Figure 6 for T-Bin. Therefore, both these findings give great confidence in the computed structures, while the latter result strongly supports the idea that Förster energy transfer (dipole−dipole interaction) from excited Trp or Bin to Toac is the most likely mechanism for the quenching process in TnTrp and T-Bin hexapeptides.[31]

Where the Dexter energy transfer model is, instead, taken into account, the results are untenable. In this case the efficiency can be written as:[21]

$$E_m/(1 - E_m) = J_D V_m{}^2/k_D \hbar^2 c \qquad (10)$$

where $k_D = \tau_0^{-1}$ is the rate constant for the donor emission, J_D the Dexter overlap integral (cm), as obtained by spectroscopic measurements, given by:

$$J_D = \int_0^\infty F_{i,D}(\bar{\nu})\epsilon_{i,A}(\bar{\nu})\, d\bar{\nu} \qquad (11)$$

with the normalization conditions:

$$\int_0^\infty F_D(\bar{\nu})\, d\bar{\nu} = \int_0^\infty \epsilon_A(\bar{\nu})\, d\bar{\nu} = 1 \qquad (12)$$

and

$$V_m{}^2 = K_m \exp(-2R_m/a) \qquad (13)$$

CHART 4: (A) Representation of the Two Chromophores in T-Bin, with Their Electric Dipole Transition Moments (Heavy Double Arrows), and (B) Geometric Arrangement Defining the Orientation between the Transition Dipole Moments of the Donor and Acceptor Molecules, and the Electric Field Vector Generated by Bin* Acting at the Center of Mass of Toac Moiety

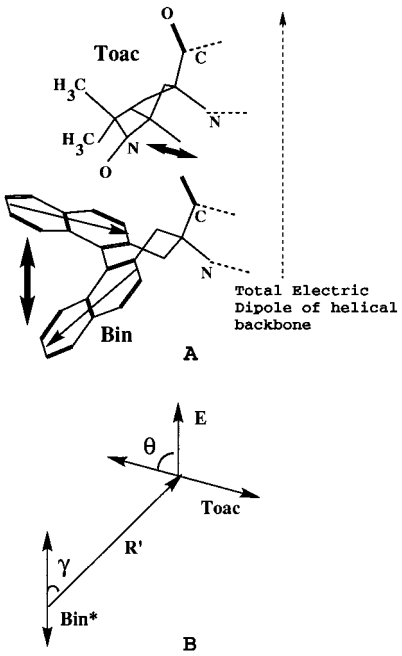

where V_m (erg) is the electronic matrix coupling element, a the average Bohr radius (0.625 Å[18b]), and K_m a quantity corresponding to the electronic matrix coupling at orbital contact. Evaluation of K_m for the peptides examined gives values in methanol that are some 5−6 orders of magnitude higher than those reported for the electronic energy transfer via exchange interaction in bichromophoric molecules,[32] spanning from 1.6×10^{-22} for T0Trp to 4.0×10^{-21} erg^2 for T3Trp, while

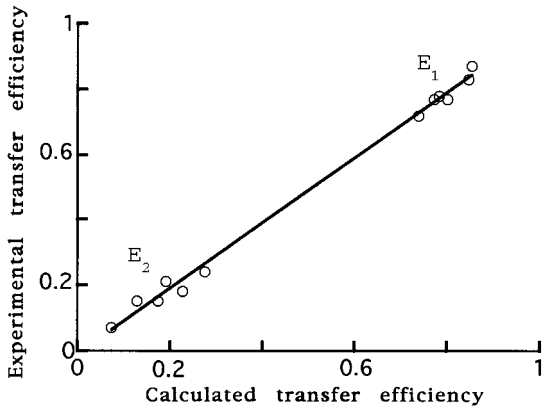

Figure 6. Comparison between experimental (eq 2) and calculated (eq 6) quenching efficiencies for T-Bin in the six solvents listed in Table 3. The two sets of points refer to the two lifetimes of the peptide. The slope of the line is 0.998.

$K_1 = 8.0 \times 10^{-23}$ and $K_2 = 7.0 \times 10^{-24}$ erg^2 for T-Bin, the latter two quantities referring to the two lifetimes of the peptide (Table 3).

Whether other mechanisms, such as electron-transfer- or electron-exchange-induced intersystem crossing to the triplet, contribute to the quenching process of Trp* or Bin* by Toac is difficult to say, but they should be definitely minor, if any.

Most Probable Structures in Solution. The results reported in Table 4 and Figure 6, showing the good agreement between observed and calculated transfer efficiencies, take implicitly into account, at least partially, the role played by the solvent medium in controlling the features of the computed structures of the peptides investigated. In fact, $E_{m,\mathrm{calcd}}$ comprises R_0 which is solvent-dependent through the values of Φ_0, τ_0, and n. Moreover, in view of the fact that the Coulombic term of eq 3 comprises the appropriate dielectric constant of the solvent, the finding that the values of P_m are close to those of α_m (Table 4)[30] points toward the same conclusion.

Taken together, these results make it reasonable to consider the energetically most favored computed structures as a good representation of those actually populating the solution.

The molecular models of the conformers of TnTrp peptides in methanol, in the deepest energy minimum, are shown in Figure 7. It is worth noting that, despite the increasing in length of the spacer, the nitroxide−indole center-to-center distance varies only slightly, at variance with the orientation parameter (Table 4), but in T2Trp. It appears, therefore, that a biased chromophore orientation contributes to the measured distance, in the sense that the two degrees of freedom of the Trp side chain are able to optimize intramolecular interactions in T0Trp, T1Trp, and T3Trp peptides at nearly the same interprobe separation distance, provided a suitable orientation between the chromophores is achieved. This implies that the mutual orientation of the chromophores is not randomized in the time scale of the quenching process, otherwise the κ_m^2 parameter should have had the isotropic average value of 0.67,[14,33] which, in turn, suggests that interconversion among conformational substates in methanol solution is definitely longer than 6 ns. A time scale much longer than 10 ns was already observed by us for the conformational substates equilibria in short helical Ala- and Aib-based peptides, carrying naphthalene and protoporphyrin IX as fluorophores, in methanol and water/methanol (75/25) solution.[14b]

On the other hand, the observation that the separation distance and orientation parameter in the most stable conformers of T2Trp are quite different from those of the other peptides in the series is very likely due to the fact that this peptide is the only one where the perpendicular and antiperpendicular conformations[23] are nearly degenerate, because of sterically favorable contacts.

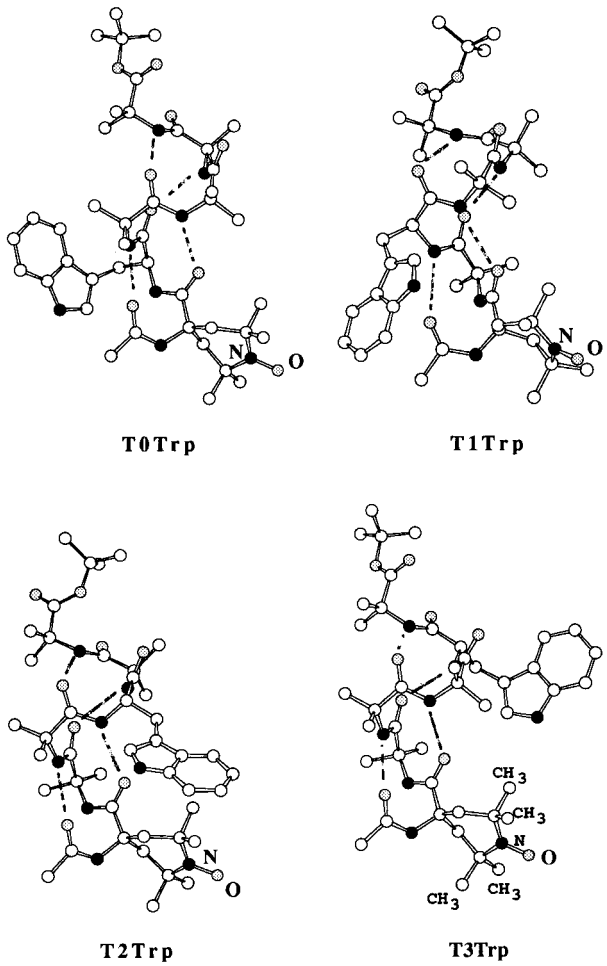

Figure 7. Molecular models of the most stable conformers of the TnTrp peptides in methanol solution. The backbone is in the right-handed 3_{10}-helix, and the four intramolecular H-bonds are indicated by broken lines. Nitrogen atoms are in black, and hydrogen atoms are omitted for clarity. In all cases, the calculated quenching efficiency, based on the molecular parameters of the models, agrees well with that experimentally determined (see Table 4).

As far as the structures of T-Bin are concerned, computational results indicate that two isoenergetic conformers with the backbone chain in the l.h. 3_{10}-helix are the energetically most favored ones, slightly more stable than the most favored conformer with the main chain in the r.h. 3_{10}-helix (Table 5). Other conformations with both helical screw senses exhibit definitely higher energies, so as to be safely neglected.

The difference between these two degenerate conformers lies on the spatial orientation of Toac with respect to Bin, owing to a different puckering of Toac moiety, as shown in Figure 8. The overall topology of Toac in the two structures is similar to that observed in the crystal state (Chart 2), the NO group pointing directly toward one naphthyl moiety of Bin. The other naphthyl moiety lies close to one methyl group of Toac (Figure 8), in such a way that the molecule can experience good H$-\pi$ interactions,[34] stiffening the whole structure. By changing the backbone screw sense, i.e., on going from l.h. to r.h. 3_{10}-helix, the spatial arrangement of the chromophores changes, causing the molecule to acquire some conformational mobility, but the ensuing gain in molecular entropy is apparently overcompen-

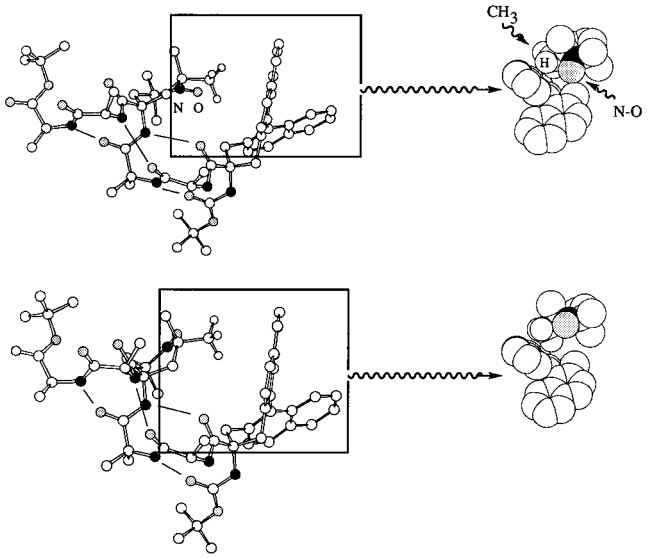

Figure 8. Molecular models of the energetically most favored conformers of T-Bin, with the backbone chain in the left-handed 3_{10}-helix (see Table 5), and the four intramolecular H-bonds indicated by thin lines. Nitrogen atoms are in black, and hydrogen atoms are omitted for clarity. Note the similarity with the crystal state structures, as determined by X-ray diffraction (Chart 2). Note also the steric arrangement of the N−O group, pointing directly toward one naphthyl moiety of Bin, while the other naphthyl moiety lies close to one methyl group of Toac, as evidenced by the space-filling model of both Toac and binaphthyl moieties. The molecule can thus experience H−π interactions that stiffen the whole structure.

sated by an increase in energy, leading to a less stable structure (Table 5).

Concluding Remarks

Combination of CD, IR, and time decay fluorescence data with molecular mechanics calculations was productive in determining the structural features in methanol solution of the hexapeptides investigated. In all cases, the molecules maintain the ordered structure and helix handedness as those present in the crystal state. The dynamics of interconversion among conformational substates in the TnTrp peptides in methanol solution is definitely longer than 6 ns, in good agreement with our earlier results on the time scale of conformational substates equilibria in short helical Ala- and Aib-based peptides in methanol and water/methanol solution.[14b]

References and Notes

(1) (a) Matko, J.; Ohki, K.; Edidin, M. *Biochemistry* **1992**, *31*, 703. (b) Matko, J.; Jenei, A.; Matyus, L.; Ameloot, M.; Damjanovich, S. *J. Photochem. Photobiol., B* **1993**, *19*, 69. (c) Matko, J.; Jenei, A.; Wei, T.; Edidin, M. *Cytometry* **1995**, *19*, 191.

(2) (a) Green, J. A.; Singer, L. A.; Parks, J. H. *J. Chem. Phys.* **1973**, *58*, 2690. (b) Green, S. A.; Simpson, D. J.; Zhou, G.; Ho, P. S.; Blough, N. V. *J. Am. Chem. Soc.* **1990**, *112*, 7337. (c) Kuzmin, V. A.; Tatikolov, A. S. *Chem. Phys. Lett.* **1977**, *51*, 45.

(3) (a) Karpiuk, J.; Grabowski, R. *Chem. Phys. Lett.* **1989**, *160*, 451. (b) Chattopadhyay, S. K.; Das, P. K.; Hug, G. L. *J. Am. Chem. Soc.* **1983**, *105*, 6205. Yee, W. A.; Kuzmin, V. A.; Kliger, D. S.; Hammond, G. S.; Twarowski, A. J. *J. Am. Chem. Soc.* **1979**, *101*, 5104.

(4) London, E. *Mol. Cell. Biochem.* **1982**, *45*, 181. Winiski, A. P.; Eisemberg, M.; Chattopadhyay, A.; London, E. *Biochemistry* **1987**, *26*, 39. Asuncion-Punzalan E.; London, E. *Biochemistry* **1995**, *34*, 11460.

(5) (a) Langner, M.; McLaughlin, S. *Biochemistry* **1988**, *27*, 386. (b) Castanho, M.; Prieto, M. *Biophys. J.* **1995**, *69*, 155. (c) Puskin, J. S.; Vistnes, A. I.; Coene, M. T. *Arch. Biochem. Biophys.* **1981**, *206*, 164.

(6) Atik, S. S,; Singer, L. A. *J. Am. Chem. Soc.* **1978**, *100*, 3234.

(7) Scaiano, J. C.; Paraskevopoulos, C. *Can. J. Chem.* **1984**, *62*, 2351.

(8) Traylor, T. G.; Sharma, V. S. *Biochemistry*, **1992**, *31*, 2847.

(9) Eiserich, J. P.; Butler, J.; Van der Vliet, A.; Cross, C. E.; Halliwell, B. *Biochem. J.* **1995**, *310*, 745.

(10) Karle, I. L.; Balaram, P. *Biochemistry* **1990**, *29*, 6747.

(11) Toniolo, C.; Benedetti, E. *Macromolecules* **1991**, *24*, 4004.

(12) Flippen-Anderson, J. L.; George, C.; Valle, G.; Valente, E.; Bianco, A.; Formaggio, F.; Crisma, M.; Toniolo, C. *Int. J. Pept. Prot. Res.* **1996**, *47* , 231. Hanson, P.; Martinez, G.; Millhauser, G.; Formaggio, F.; Crisma, M.; Toniolo, C.; Vita, C. *J. Am. Chem. Soc.* **1996**, *118*, 271.

(13) Pispisa, B.; Venanzi, M.; D′Alagni *Biopolymers* **1994**, *34*, 435. Pispisa, B.; Venanzi, M.; Palleschi, A. *Faraday Trans.* **1994**, *90*, 1857.

(14) (a) Pispisa, B.; Venanzi, M.; Palleschi, A.; Zanotti, G. *J. Mol. Liquids* **1994**, *61*, 167. Pispisa, B.; Venanzi, M.; Palleschi, A.; Zanotti, G. *Macromolecules* **1994**, *27*, 7800. Pispisa, B.; Venanzi, M.; Palleschi, A.; Zanotti, G. *Biopolymers* **1994**, *36*, 497. Pispisa, B.; Palleschi, A.; Venanzi, M.; Zanotti, G. *J. Phys. Chem.* **1996**, *100*, 6835. (b) Pispisa, B.; Venanzi, M.; Palleschi, A.; Zanotti, G. *J. Photochem. Photobiol., A: Chem.* **1997**, *105*, 225. (c) Pispisa, B.; Palleschi, A.; Amato, M. E.; Segre, A. L.; Venanzi, M. *Macromolecules* **1997**, *30*, 4905.

(15) Flippen-Andersen, J. L.; George, C.; Graci, L.; Formaggio, F.; Crisma, M.; Toniolo, C. To be published.

(16) Toniolo, C,; Formaggio, F.; Crisma, M.; Mazaleyrat, J. P.; Wakselman, M.; George, C.; Flippen-Andersen, J. L.; Pispisa, B.; Venanzi, M.; Palleschi, A. In *Proceedings of the 15th American Peptide Symposium*; Tam, J. P., Kaumara, P. T. P., Eds; Kluwer: Dordrecht, The Netherlands, in press.

(17) Förster, T. *Discuss. Faraday Soc.* **1959**, *27*, 7.

(18) (a) Scholes, G. D.; Ghiggino, K. P.; Oliver, A. M.; Paddon-Row: M. N. *J. Am. Chem. Soc.*, **1993**, *115*, 4345. (b) Scholes, G. D.; Ghiggino, K. P. *J. Phys. Chem.* **1994**, *98*, 4580.

(19) Woody, R. W. In *Circular Dichroism: Principles and Applications*; Nakanishi, K., Berova, N., Woody, R. W., Eds; VCH; New York, 1994; pp 473−496.

(20) Pispisa, B.; Cavalieri, F.; Venanzi, M.; Sisto, A. *Biopolymers* **1996**, *40*, 529, and references therein.

(21) Dexter, D. L. *J. Chem. Phys.* **1953**, *21*, 836.

(22) Allinger, N. L. *J. Am. Chem. Soc.* **1977**, *99*, 8127. Burkert, J.; Allinger, N. L. *Molecular Mechanics*; American Chemical Society: Washington, D. C., 1982.

(23) Willis, K. J.; Szabo, A. G. *Biochemistry* **1992**, *31*, 8924.

(24) Benedetti, E.; Morelli, G.; Nemethy, G.; Scheraga, H. A. *Int. J. Pept. Protein Res.* **1983**, *22*, 1. Vasquez, M.; Nemethy, G.; Scheraga, H. A. *Macrololecules* **1983**, *16*, 1043.

(25) (a) Pispisa, B.; Palleschi, A.; Barteri, M.; Nardini, S. *J. Phys. Chem.* **1985**, *89*, 1767. Pispisa, B.; Palleschi, A.; Paradossi, G. *J. Phys. Chem.* **1987**, *91*, 1546. Pispisa, B.; Paradossi, G.; Palleschi, A.; Desideri, A. *J. Phys. Chem.* **1988**, *92*, 3422; (b) Paradossi, G.; Chiessi, E.; Venanzi, M.; Pispisa, B.; Palleschi, A. *Int. J. Biol. Macromol.* **1992**, *14*, 73. Chiessi, E.; Branca, M.; Palleschi, A.; Pispisa, B. *Inorg. Chem.* **1995**, *34*, 2600.

(26) (a) Steinberg, I. Z. *J. Chem. Phys.* **1968**, *48*, 2411. (b) Grinvald, A.; Haas, E.; Steinberg, I. Z. *Proc. Natl. Acad. Sci. U.S.A.* **1972**, *69*, 2273.

(27) Hol, W. G. J.; van Duijnen, P. T.; Berendesen, H. J. C. *Nature* **1978**, *273*, 443.

(28) Fox, M. A.; Galoppini, E. *J. Am. Chem. Soc.* **1997**, *119*, 5277.

(29) (a) Callis, P. R. *J. Chem. Phys.* **1991**, *95*, 4230. (b) Lami, H.; Glasser, N. *J. Chem. Phys.* **1986**, *84*, 597. Lipinski, J.; Chojnacki, H. *Spectrochim. Acta* **1995**, *51A*, 381.

(30) In the absence of static quenching, the relationship between the pre-exponentials in the decay and the normalized molecular fraction of the mth conformer in the ground state, P_m, is as follows: $\alpha_m = (f_m/\tau_m)/\sum_m(f_m/\tau_m) = (P_m\Phi_m/\tau_m)/\sum_m(P_m\Phi_m/\tau_m) = [P_m(\Phi_0/\tau_0)]/\sum_m[P_m(\Phi_0/\tau_0)] = P_m$, where $\Phi_m/\Phi_0 = \tau_m/\tau_0$, $f_m = \alpha_m\tau_m/\sum_m\alpha_m\tau_m$ is the fluorescence fraction, and τ_0 and Φ_0 are the lifetime and quantum yield of the nonquenched chromophore, respectively. For a multiexponential decay, the lack of static quenching implies that $\langle\tau\rangle/\tau_0 = \Phi/\Phi_0$, where $\langle\tau\rangle = \sum_m\alpha_m\tau_m$, as obtained by integrating eq 1. Owing to the large errors in evaluating $\langle\tau\rangle$, because of the three lifetime components and the associated uncertainties (Table 2), one must be very careful in comparing $\langle\tau\rangle/\tau_0$ and Φ/Φ_0. In all peptides examined, but T-Bin and possibly T2Trp, static quenching is definitely minor, if any. This is because the steric arrangement of the probes in these molecules is such as to prevent any instantaneous process within a complex between the active chromophores. In fact, all conformers of both T0Trp and T1Trp exhibit a center-to-center distance larger than 6.5 Å (Table 4), while the helical periodicity is such that the NO and Trp groups lie on the opposite sides of the helical backbone, as shown in Figure 7. A static quenching can be thus ruled out on purely steric grounds. Accordingly, within experimental errors $\langle\tau\rangle/\tau_0 = \Phi/\Phi_0$, i.e., $\langle\tau\rangle/\tau_0 = 0.08 \pm 0.04$ vs $\Phi/\Phi_0 = 0.04 \pm 0.02$ for T0Trp and 0.08 ± 0.05 vs 0.10 ± 0.04 for T1Trp. The same conclusion can be drawn for T3Trp, whose conformers have an interprobe distance still larger than 6.5 Å. Furthermore, although the chromophores lie on the same side of the helix (Figure 7), there is a methyl group of Toac inbetween NO and Trp that prevents a close approach of these chromophores, making any instantaneous process very unlikely. In this connection, it is worth noting that both intermolecular[1a,5b] and intramolecular experiments[2b] involving a

nitroxide quencher have recently shown that static quenching is negligible or absent, even though the center-to-center distance was as short as 6.5 Å.[2b] By contrast, the finding that both the difference between $\langle\tau\rangle/\tau_0$ and Φ/Φ_0 is beyond experimental errors in T2Trp and the two most populated conformers of this peptide exhibit the shortest center-to-center distance among all compounds examined ($R_m = 5.7$ and 6.0 Å) suggests that some static quenching occurs. On the other hand, the stereochemical features of the chromophores in T-Bin (Figure 8) are also likely to favor a static quenching in that the NO group points directly toward Bin, at a separation distance of 5.8 and 6.2 Å, depending on the structure (Table 5). Accordingly, the difference between $<\tau>/\tau_0$ and Φ/Φ_0 is well beyond experimental errors. To summarize, static quenching can be ruled out for T0Trp, T1Trp, and T3Trp, and the good (qualitative) agreement between α_m and P_m fulfils this condition. On the contrary, it does occur in T-Bin, while there is some uncertainty for T2Trp, this peptide probably lying inbetween the former compounds and T-Bin because its values of α_m and P_m are still comparable.

(31) Förster, T. *Ann. Phys.* (*Leipzig*) **1948**, *2*, 55.

(32) Speiser, S.; Katriel, J. *Chem. Phys. Lett.* **1983**, *102*, 88. Hassoon, S.; Lustig, H.; Rubin, M. B.; Speiser, S. *J. Phys. Chem.* **1984**, *88*, 6367.

(33) (a) McWherter, C. A.; Haas, E.; Leed, A. R.; Scheraga, H. A. *Biochemistry* **1986**, *25*, 1951. (b) Valeur, B.; Mugnier, J.; Pouget, J.; Bourson, J.; Santi, F. *J. Phys. Chem.* **1989**, *93*, 6073.

(34) (a) Malone, J. F.; Murray, C. M.; Charlton, M. H.; Docherty, R.; Lavery, A. J. *J. Chem. Soc., Faraday Trans.* **1997**, *93*, 3429, and references therein. (b) Rozas, I.; Alkorta, I.; Elguero, J. *J. Phys. Chem.* **1997**, *101*, 9457.